

Polar-molecules-driven enhanced colloidal electrostatic interactions and their applications in achieving high active electrorheological materials

L. Xu,^{a)} W.J. Tian,^{a)} X.F. Wu, J.G. Cao, L.W. Zhou, and J.P. Huang^{b)}
*Surface Physics Laboratory and Department of Physics, Fudan University,
Shanghai 200433, People's Republic of China*

G.Q. Gu

*School of Information Science and Technology, East China Normal University,
Shanghai 200062, People's Republic of China*

(Received 2 August 2007; accepted 16 October 2007)

We have fabricated a class of colloidal electrorheological (ER) fluids, in which suspended TiO₂ particles were synthesized by a sol-gel method and modified by 1,4-butyrolactone molecules with a permanent molecular dipole moment of 4.524 D. Compared with pure TiO₂ ER fluids, the quasi-static yield stress of the polar-molecules-modified ER fluid is enhanced as high as 48.1 kPa when subjected to an external electric field of 5 kV/mm. Also, it possesses other attractive characters such as low current density (<14 μA/cm²) and low sedimentation. Based on a Green's function method, we present a first-principles approach to investigate colloidal electrostatic interactions. Excellent agreement between experiment and theory has been shown for the enhancement ratio of quasi-static yield stress, which quantitatively reveals that enough polar molecules oriented within the field-directed gap between the colloidal particles can unexpectedly enhance the interactions, thus yielding the unusual enhancement. This shows a promising and flexible direction for achieving more highly active ER materials.

I. INTRODUCTION

If interparticle interactions are determined or tailored, the macroscopic structures of various materials or systems can be realized accordingly, which may possess desired optimal physical or chemical properties.^{1–8} Thus, the study of interparticle interactions is of particular importance. In this work, we report a kind of enhanced colloidal electrostatic interaction driven by polar molecules. As an application, we shall fabricate a class of colloidal electrorheological (ER) fluids composed of TiO₂ particles modified by 1,4-butyrolactone molecules with permanent molecular dipole moment 4.524 D (1 D ≈ 3.33564 × 10⁻³⁰ C·m). The highly active properties of the ER fluids will be characterized and confirmed.

ER fluids are a suspension composed of polarizable colloidal particles dispersed in an insulating carrier fluid.^{9–26} The flow properties of ER fluids can be controlled by an electric field.^{9–26} They can be transformed

into a solid-like state when an electric field is applied, and the transition is reversible as the electric field is turned off.⁹ This phenomenon is expected to be widely used in different industries¹⁰ (e.g., in active control of conventional and intelligent devices). Owing to the insufficient performance of ER fluids, research on highly active ER materials for practical technical applications have been a challenge over the last decade.^{9–26} Generally, the ER particles are micrometer- or nanometer-sized. Recently, it was found that the optimal ER materials are nanometer-sized particles^{11,14} or micrometer-sized particles with nanometer-sized structures, such as pores or layers.^{15,17} The polar-molecular dominated ER effect²⁵ was proposed to explain the high ER effect of polar molecules absorbed ER fluids. These ER fluids show more advantages such as large shear stress, low current density, and low sedimentation.

TiO₂ is a popular material with a high-dielectric constant that is easy to manufacture; it has been the subject of many investigations. But, the pure TiO₂ ER fluid shows a rather low yield stress (e.g., 0.6 kPa in an electric field of 4 kV/mm).¹⁵ By using a double layer coating of TiO₂-Ni, Tam et al.¹⁸ created an ER fluid whose yield stress was enhanced to a few orders of magnitude over the pure TiO₂ ER fluid. It is said that the modification of

^{a)}L. Xu and W.J. Tian have contributed equally to this work.

^{b)}Address all correspondence to this author.

e-mail: jphuang@fudan.edu.cn

DOI: 10.1557/JMR.2008.0057

the nanometer-sized particles or nanometer-sized structures plays a crucial role in the enhancement of ER responses.

In this work, we shall fabricate an ER fluid composed of organic modified titanium dioxide (i.e., 1,4-butyrolactone–TiO₂). The concentration of the ER fluids is denoted by the ratio of the volume of the base oil (in milliliters) to the mass of the powder (in grams)¹⁹ (the ratio will be called the “liquid–solid ratio”; i.e., 1 g of the powder mixed with 0.45 mL of silicon oil is denoted as 0.45 mL/g). The experimental results show that the yield stress (which is used to represent “quasi-static yield stress” in both our experiment and theory throughout this work) reaches 48.1 kPa for an external electric field of 5 kV/mm and a liquid–solid ratio 0.45 mL/g. The sedimentation ratio of the polar-molecules-modified ER fluids is >99% after 500 h of testing. These properties may satisfy many industrial applications nowadays. To this end, the physical mechanism behind the enhanced yield stress will be analyzed by using a first-principles approach based on a Green’s function method. As a result, the enhanced yield stresses are, indeed, found to appear due to polar-molecules-driven enhanced colloidal electrostatic interactions.

II. EXPERIMENTS

A. Preparation of 1,4-butyrolactone-modified TiO₂ particles

The 1,4-butyrolactone–TiO₂ gel powders were prepared by a sol-gel method. 1,4-Butyrolactone and titanium butoxide [Ti(C₄H₉O)₄] were used as raw materials. Acetic acid (HAc, CH₃COOH), ethanol (C₂H₅OH), and deionized water were used as solvents. Ti(C₄H₉O)₄ was dissolved in ethanol at a volume ratio of Ti(C₄H₉O)₄/ethanol = 1:2, in which a small amount of acetic acid was added to avoid precipitation. On the other hand, a solution of 1,4-butyrolactone and deionized water was mixed in ethanol, and then added into the Ti(C₄H₉O)₄ solution. The sol was kept in air at room temperature to form a gel. The 1,4-butyrolactone-modified TiO₂ gel particles were obtained by drying the gel in an oven at 75 °C for 72 h. A group of modified TiO₂ particles was prepared with a different volume of 1,4-butyrolactone.

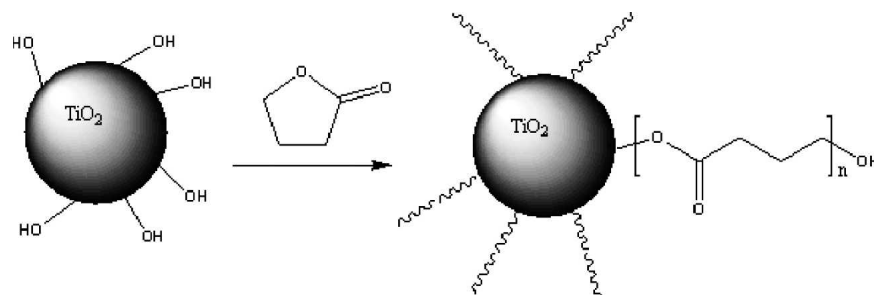


FIG. 1. A schematic graph showing the possible sol-gel process of 1,4-butyrolactone and titanium butoxide along with chemical reaction routes.

Besides that, the TiO₂ sample was synthesized without doping in the same way for purposes of comparison.

B. Preparation of ER fluids

The host insulating oil used in the ER fluids was silicone oil whose dielectric constant was 2.5, density was 0.965 g/cm³, and viscosity was 50 mPa*s at a room temperature of 25 °C. The dried samples were mixed quickly with the silicone oil. The mixed suspension was milled for 2 h in a mortar and then heated at 60 °C for 2 h.

C. Characterization

The microstructure and particle size of the gels were examined by scanning electron microscopy (SEM) and submicron particle size analyzer. The ER effect was characterized by the yield stress under direct current (dc) electric fields. The experimental data were collected by a Mecmesin (West Sussex, UK) torque indicator with two parallel plates. The diameter of the plate was 20 mm, and the gap between two plates was 1.0 mm. The quasi-static shear stress was measured at a relatively low shear rate of 0.06 s⁻¹.

III. EXPERIMENTAL RESULTS

A. Material characteristics

A schematic graph showing the possible sol-gel process of 1,4-butyrolactone and titanium butoxide along with chemical reaction routes is seen in Fig. 1. And the x-ray diffraction (XRD) of the 1,4-butyrolactone-modified TiO₂ particles is shown in Fig. 2. There is no sharp characteristic peak but there are wide wave packets, which suggest the existence of an amorphous pattern. The particle size distribution was tested by the N4 Plus submicron particle size analyzer (Beckman Coulter Co., Brea, CA), and the spectrum is shown in Fig. 3. The average powder diameter generated by the apparatus was 919.4 nm. The SEM images in Fig. 4 indicate irregular particle morphology, and the powder diameter ranges from nanometers to micrometers in Fig. 4(a), which accords with the size distribution seen in Fig. 3. The particles consist of nanoparticles, which aggregated to show irregular morphology. The gel was dried at a temperature of 75 °C, which is quite low and thus makes it difficult to

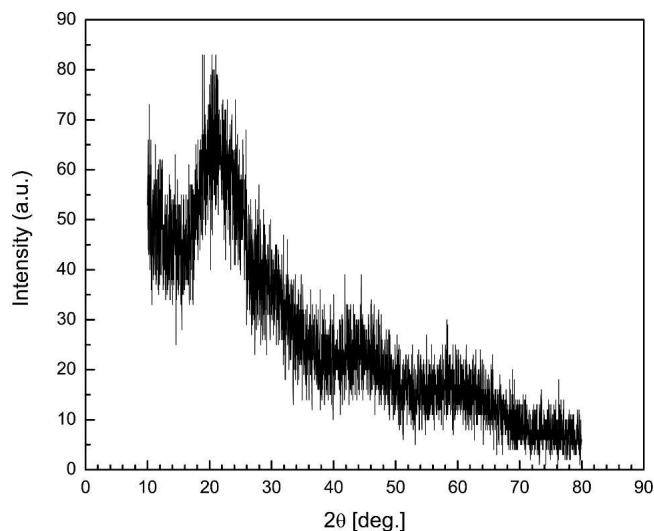


FIG. 2. XRD pattern of 1,4-butyrolactone-modified TiO_2 particles.

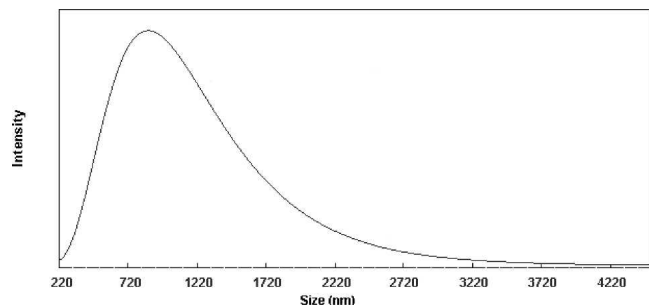
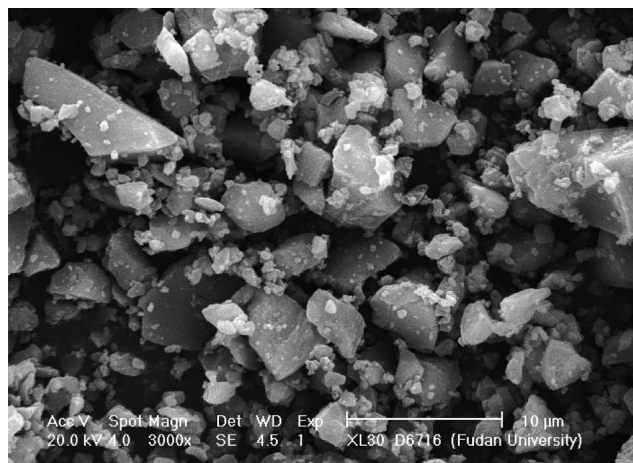


FIG. 3. The diameter distribution of 1,4-butyrolactone-modified TiO_2 particles.

format the rutile or anatase phase. The XRD suggests that the pattern of our sample is amorphous. On the other hand, the sample was milled, so it is likely to aggregate during the process of milling. Under the high resolution shown in Fig. 4(b), both small particles and large agglomerated particles can be seen.

Figure 5 gives the infrared spectra of [Fig. 5(a)] 1,4-butyrolactone-modified TiO_2 particles and [Fig. 5(b)] bare TiO_2 particles (which was also made by the similar sol-gel method). The broad band near 3550 cm^{-1} indicates the O–H stretching vibration and alkane C–H stretching absorptions just below 3000 cm^{-1} demonstrate the presence of saturated carbons. The TiO_2 structure is well recognized by the presence of Ti–O stretching vibration in the 487-cm^{-1} region. These peaks can be found in both samples. Along with the Fourier transform infrared (FTIR) spectra of pure 1,4-butyrolactone, the strong peaks of 1777 cm^{-1} (carbonyl group) and 1172 cm^{-1} (C–O bond) coordinate with the spectra of the modified TiO_2 particles. The peak near the 1735-cm^{-1} region indicates the presence of a carbonyl group, and the peaks in the region of $1050\text{--}1300\text{ cm}^{-1}$ demonstrate the presence of the C–O bond. These can only be found in



(a)



(b)

FIG. 4. SEM images of 1,4-butyrolactone-modified TiO_2 particles.

the modified sample, so the presence of the 1,4-butyrolactone-modified TiO_2 is confirmed.

B. Rheological properties of the prepared ER fluids

The curves of the yield stress and current density of the prepared ER fluids of amorphous 1,4-butyrolactone-modified TiO_2 particles suspended in silicone oil under different electric fields are shown in Fig. 6. We adopted dc voltage in our experiment in view of the possible industrial applications. In some studies (e.g., Wen et al.¹⁹), the yield stress of giant ER fluids was measured by using square-wave voltage pulses because they are easier to observe and can avoid large amounts of leaking current. The reported nano-ER materials¹⁹ with high yield stress show a slow response time, longer than 1 s. For our ER fluids of 1,4-butyrolactone-modified TiO_2 , the data on yield stress were collected every 10 ms, which indicates that the response time is at least $<10\text{ ms}$.

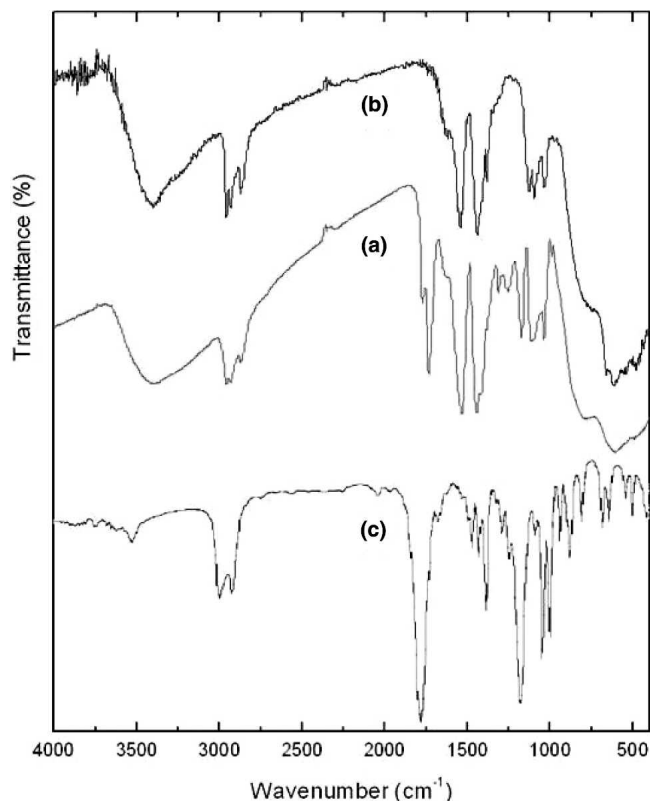


FIG. 5. The FTIR spectra of (a) 1,4-butyrolactone-modified TiO_2 , (b) bare TiO_2 (which was also made by the sol-gel method for comparison), and (c) the standard spectra of pure 1,4-butyrolactone.

Under a relatively low electric field, the yield stress shows a square relation with the external electric field. When the electric field exceeds 1.5 kV/mm, the relation becomes linear. Meanwhile, the current density is quite low, $<14 \mu\text{A}/\text{cm}^2$ in the presence of an applied external field of 5 kV/mm.

Several samples with different volumes of 1,4-butyrolactone were synthesized, and their yield stresses were tested at the same liquid–solid ratio of 0.5 mL/g. The best ER performance appears when the mole ratio of 1,4-butyrolactone versus titanium butoxide is about 1.5. The yield stress and current density of this sample are shown in Fig. 6, and the yield stress is larger than that seen in Fig. 7 for the cases in which the mole ratios are >1.5 . When the mole ratio is <1.5 , the yield stress grows with the increase in 1,4-butyrolactone. When the mole ratio is >1.5 , the yield stress decreases. Simultaneously, the ability to endure electric fields declines, as shown in Fig. 7. The curves illustrate clearly that when the volume of 1,4-butyrolactone increases to some degree, a higher electric field is impossible to apply.

We have also measured the shear stress versus the shear rate (Fig. 8). Figure 8 shows that the increase in shear rate causes the shear stress to decrease, which is due to the reduction of the polarization of the dynamic suspended particles.²⁰

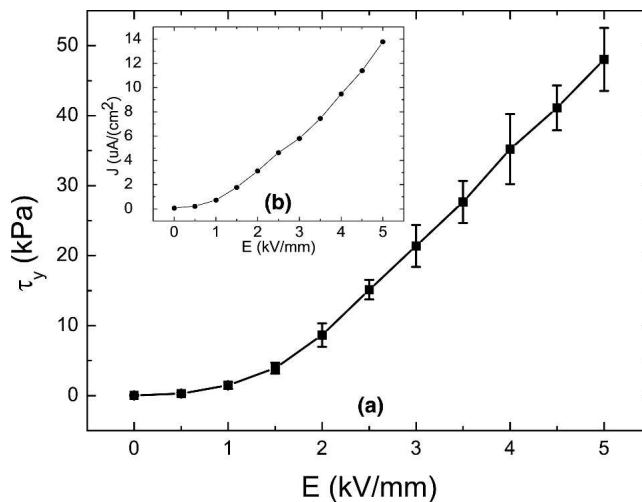


FIG. 6. Yield stress τ_y and current density J of the prepared ER fluid, with a liquid–solid ratio of 0.45 mL/g and a mole ratio (1,4-butyrolactone/titanium butoxide) of 1.5, of 1,4-butyrolactone-modified TiO_2 particles suspended in silicon oil, as a function of dc electric fields. The accuracy of yield stress versus electric field is also shown. At each certain electric field, we kept a record of the first 30 to 40 pieces of data that were output and then calculated the average value. The standard deviation of each value is indicated.

C. Dielectric properties of the prepared ER fluids

Because it is difficult to directly measure the dielectric properties of the suspended particles, the 1,4-butyrolactone-modified TiO_2 powder was pressed into a thin disk (2 mm thick and 14 mm in diameter). The capacitance C and conductance G were obtained using a Hewlett Packard (Palo Alto, CA) 4284A precision LCR meter. The relative dielectric constant of the particles (ϵ) was derived from the measured C according to the conventional relation, $\epsilon = Cd/(\epsilon_0 S)$, where $\epsilon_0 = 8.854 \times 10^{-12}$ F/m is the dielectric constant of the vacuum and d

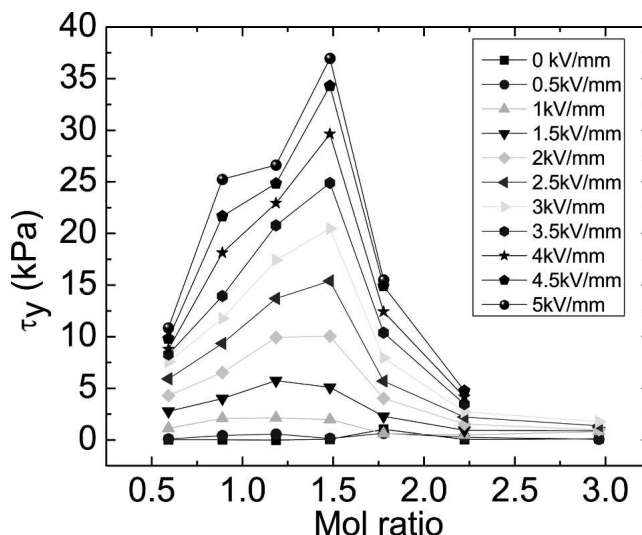


FIG. 7. Yield stress τ_y versus 1,4-butyrolactone/titanium butoxide mole ratios for different electric fields. All of the liquid–solid ratios used are 0.5 mL/g.

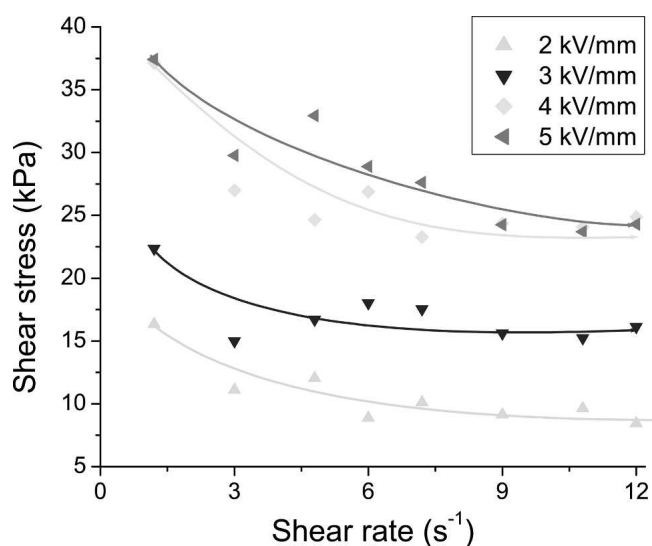


FIG. 8. Shear stress versus shear rate for the prepared ER fluid, with liquid–solid ratio of 0.45 mL/g and a mole ratio (1,4-butyrolactone/titanium butoxide) of 1.5 for 1,4-butyrolactone-modified TiO₂ particles suspended in silicon oil for four different electric fields: 2, 3, 4, and 5 kV/mm. Solid lines serve respectively as visual guides.

and S are the thickness and area of the powder disk, respectively. ϵ decreases dramatically with frequency and approaches a constant value at high frequency under a fixed field strength (Fig. 9). The conductivity of the particles (σ) was calculated with measured G according to the relation $\sigma = Gd/S$.

It is widely accepted that the Wagner interfacial polarization is responsible for the interaction force that leads to the rheological change in the ER fluids.²¹ This mechanism treats particle polarization by the complex constant, $\epsilon = \epsilon' - i\epsilon''$, where the real part ϵ' is related to polarizability and the imaginary part ϵ'' is related to the dielectric loss, which can also be expressed as $\sigma/(2\pi f)$.

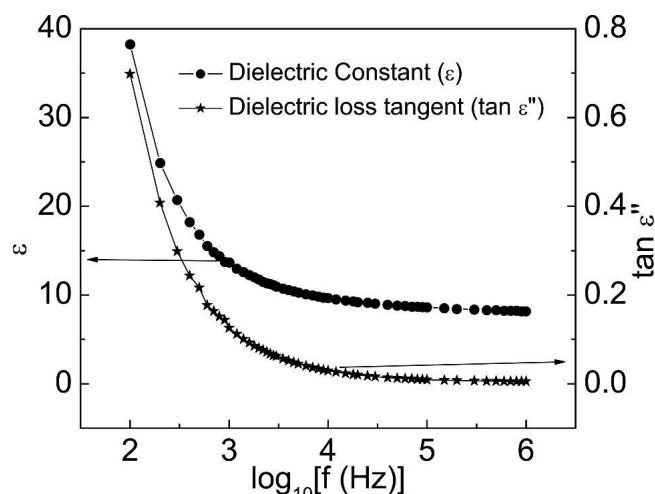


FIG. 9. The dielectric properties of 1,4-butyrolactone-modified TiO₂ particles versus the frequency f of the external field.

Here, σ denotes the conductivity, and f denotes the frequency of the external field. Hao et al.²² further proposed that a good ER effect requires an electric relaxation peak in ϵ'' between 10² and 10⁵ Hz as well as a large $\Delta\epsilon'$ ($\Delta\epsilon' = \epsilon'_{100\text{Hz}}/\epsilon'_{1\text{MHz}}$).²² However, in the ER fluids that we prepared, we also noticed that there was no dielectric relaxation peak between 10² and 10⁶ Hz in the 1,4-butyrolactone-modified TiO₂ (see Fig. 9). However, the fluids possessed high ER activity as well.

D. Sedimentation stability of ER fluids

When the density of the particles is not the same as that of the medium, the particles with micrometer-order size will settle down²⁷ according to Stoke's law. To solve the traditional problem of particle sedimentation, different solutions have been developed.^{23,28} The density mismatch between gels and the continuous phase plays an important role in the sedimentation ratio of the ER fluid. The sedimentation stability of the prepared ER fluids of 1,4-butyrolactone-modified TiO₂ particles suspended in silicon oil is excellent, and the sedimentation ratio is >99% after 500 h of testing.

The high stability of suspensions against sedimentation has been demonstrated, and the particle size is on the order of 1 μm , as shown in Fig. 3. In addition, the density of TiO₂ is >3.5 g/cm³ under ordinary conditions. From these data, the suspensions can be flocculated by colloidal attraction even in zero fields. However, in the analysis of electric forces in ER suspensions, it is generally assumed that the systems are dispersed by noninteracting particles in zero fields. Interestingly, if the suspensions are flocculated by nonelectric forces (e.g., colloidal attraction), the ER behavior often shows the hysteresis effect, as shown in Fig. 10. In other words, Fig. 10 shows that colloidal attraction exists in our system. On the other hand, the yield stress after the removal of electric fields is shown to deviate slightly from zero (see Fig. 10), which also shows that colloidal attraction exists in the zero field.

IV. THEORY: MECHANISM ANALYSIS

We are now in a position to understand the physical mechanism under the enhancement of yield stresses in the prepared ER fluids with TiO₂ particles modified by 1,4-butyrolactone. In our experiment, 1,4-butyrolactone has a molecular dielectric dipole moment, p_0 , of about 4.524 D. Recently, Lu et al.²⁵ studied the influence of dipoles between particles. Obviously, the permanent molecule dipole moments of 1,4-butyrolactone can be directed along the direction of the local electric field as long as the field is strong enough. Here, we shall investigate the effect of dipoles between the particles on the electrostatic interaction between the particles in an attempt to interpret the significantly enhanced yield stress

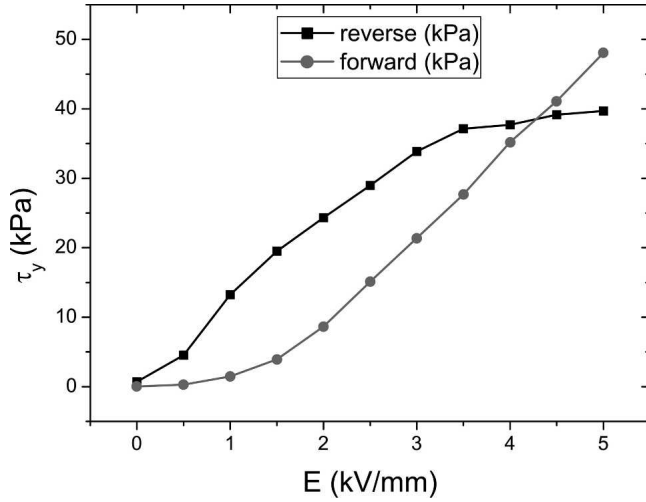


FIG. 10. The yield stress τ_y versus the electric field E as E increases from 0 to 5 kV/mm (indicated as “forward”), or decreases from 5 to 0 kV/mm (indicated as “reverse”), measured for the prepared ER fluid with a liquid–solid ratio of 0.45 mL/g and a mole ratio (1,4-butyrolactone/titanium butoxide) of 1.5 for 1,4-butyrolactone-modified TiO_2 particles suspended in silicon oil. The hysteresis effect is clearly shown.

reported in our experiment. To this end, we find that enough polar molecules can strengthen colloidal electrostatic interaction significantly, which thus leads to the unusual enhancement of yield stresses.

To simplify, we focus on two stationary particles, which are modified by 1,4-butyrolactone or not, suspended in the carrier liquid. This is because the yield stress theoretically predicted for two touching particles is expected to be approximately proportional to that experimentally measured for the whole ER fluid system, due to the dominance of two-body interactions over many-body interactions.²⁹ For a pair of bare particles, we can calculate the energy and then obtain the interaction force between the two particles.³⁰ In this work, we should take into account the effect of polar molecules between the particles (or equivalently, oriented within the field-directed gap between them), beyond which such an effect can be neglected due to the symmetry. According to the Green’s function approach, the effects of charges on the potential at any position can be written as

$$\Phi(\mathbf{r}) = -E_0 z + \frac{1}{4\pi} \int q(\mathbf{r}') G(\mathbf{r} - \mathbf{r}') d\mathbf{r}' \quad , \quad (1)$$

where $q(\mathbf{r}')$ includes the surface-polarized charges induced by an electric field and the intrinsic dipoles (of the polar molecules) oriented within the gap between the particles. Here, the intrinsic dipoles tend to be directed along the direction of the local electric field. The effective dipole moment of all the intrinsic dipoles may be related to the Langevin function [see Eq. (7) below]. The local electric field E_{loc} at the center of the gap between the two particles is

$$E_{\text{loc}} = \frac{16(\epsilon - \epsilon_h)a^3 + (\epsilon + 2\epsilon_h)R^3}{3R^3\epsilon_h} C_1 \quad , \quad (2)$$

which is up to the first order. In this equation, a is the radius of a particle, R is the center-to-center distance between the two particles, and ϵ (or ϵ_h) is the dielectric constant of the TiO_2 particle (or host oil). Because the local field decreases rapidly from the center (maximal strength) to the periphery of the gap (minimal strength), we can simply assume that an effective dipole moment, p , along the direction of the local field is induced to appear at the center. As a result, the parameter C_1 in Eq. (2) is determined by the Rayleigh identities, which are related to the properties of both particles. In this case, we have

$$C_1 = \frac{12p - 3E_0\pi R^3\epsilon_h}{\pi[(\epsilon - \epsilon_h)a^3 + (\epsilon + 2\epsilon_h)R^3 - 3(\epsilon - \epsilon_h)a^3 \cos^2\theta]} \quad . \quad (3)$$

We will find later that the p is responsible for the enhanced yield stress. Here, θ denotes the shear strain, namely, an angle by which the two particles are sheared, relative to the applied field direction.

The change in electrostatic energy due to the introduction of particles (TiO_2) and polar molecules (1,4-butyrolactone) into the host medium in the presence of an external electric field, \mathbf{E}_0 , is

$$W = \frac{1}{8\pi} \sum_{\gamma=\alpha,\beta} \int_{\Omega_p} (\epsilon_h - \epsilon_\gamma) \mathbf{E}_{\text{loc}} \cdot \mathbf{E}_0 dx^3 + \mathbf{p} \cdot \mathbf{E}_{\text{loc}} \quad . \quad (4)$$

Here, ϵ_α and ϵ_β represent the dielectric constant of particle α and particle β , respectively. In this work, there is $\epsilon_\alpha = \epsilon_\beta \equiv \epsilon$. By solving the potential from the Laplace equation, the change in energy due to particles is given by

$$W = \frac{1}{3}(\epsilon - \epsilon_h)a^3 C_1 E_0 + p E_{\text{loc}} \quad . \quad (5)$$

Consequently, we can get the stress $\tau(\theta)$ between the two particles by deviating Eq. (5) with respect to θ ,

$$\begin{aligned} \tau(\theta) &= -\frac{1}{V} \frac{\partial W}{\partial \theta} \\ &= -\frac{1}{V} \frac{6a^3(\epsilon - \epsilon_h)(\pi\epsilon_h R^3 E_0 - 4p)\Omega \cos\theta \sin\theta}{\pi\epsilon_h R^3 \left[a^3(\epsilon - \epsilon_h) + R^3(\epsilon + 2\epsilon_h) \right]^2 - 3a^3(\epsilon - \epsilon_h) \cos^2\theta} \quad , \end{aligned} \quad (6)$$

with $\Omega = a^3(\epsilon - \epsilon_h)(R^3\epsilon_h E_0 + 16p) + R^3(\epsilon + 2\epsilon_h)p$, where V is the average volume occupied by a particle (modified by 1,4-butyrolactone). This result is approximate to the first order. The complete analytic result including all higher orders is much more complex, and this result (up to the first order) is already good enough to interpret the experimental result due to its dominance.

V. COMPARISON BETWEEN EXPERIMENT AND THEORY

For the exponent of the yield stress versus electric field, a polarization model, conduction model, and polar-molecule-dominated ER model give 2.0, 1.5, and 1.0, respectively.³¹ According to our experimental result that is displayed in Fig. 11(a), the exponent is ~ 2.0 when the electric field is weak (i.e., <1.5 kV/mm) [Fig. 11(a)], and ~ 1.0 when the applied field is strong (i.e., >1.5 kV/mm) [Fig. 11(b)]. Regarding the situation seen in Fig. 11(a), it is because in weak fields the number of effective polar molecules is small. We can also see in Eq. (6) that when $p \ll R^3 \epsilon_h E_0$, the yield stress is proportional to E_0^2 , with

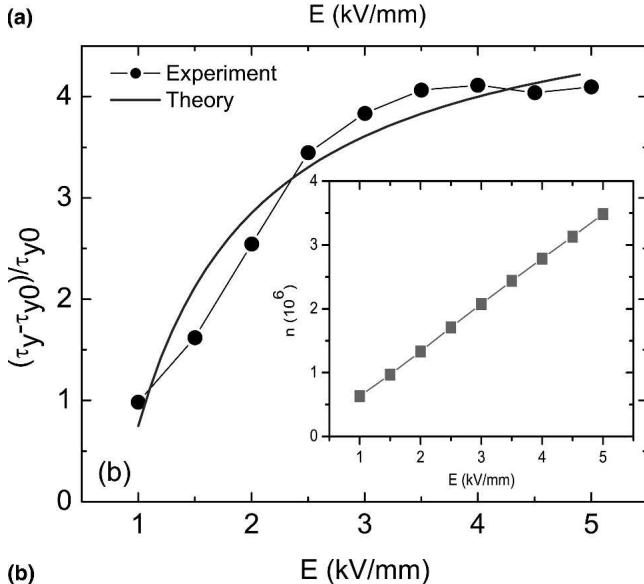
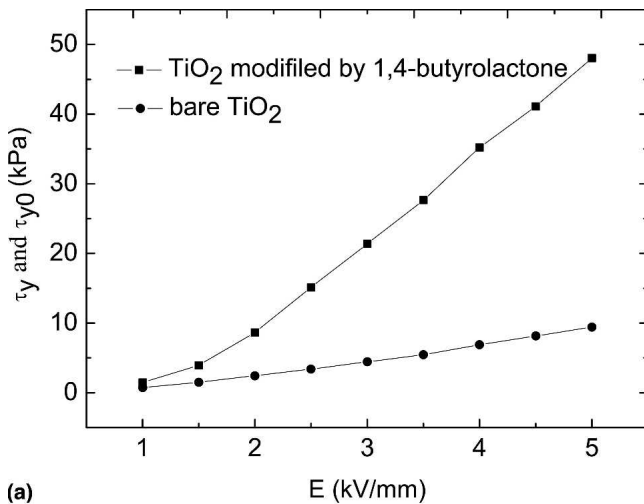


FIG. 11. (a) Experimental result for yield stresses τ_y and τ_{y0} . τ_y : TiO_2 modified by 1,4-butyrolactone (with liquid–solid ratio of 0.45 mL/g or a mole ratio of 1.5). τ_{y0} : bare TiO_2 . (b) Theoretical fitting of the enhancement ratio of yield stress, $(\tau_y - \tau_{y0})/\tau_{y0}$, to external electric fields. Symbols correspond to the experimental results already shown in (a). The inset shows the number n of polar molecules (dipoles) within the gap between the two particles as a linear function of external electric fields according to Eq. (7), which is used for the theoretical fitting.

the exponent being 2.0. This case can be described in a polarization-dominated model. Regarding Fig. 11(b), for high E_0 , the effect of polar molecules increases, and the relation between the dipole moment p and the electric field E_0 determines the exponent. In this case, the exponent 1.0 is shown in our experiment, which reveals that the system of our interest is dominated by polar molecules.

Figure 11(a) displays the experimental results for the yield stress τ_y of TiO_2 particles modified by 1,4-butyrolactone and the τ_{y0} of bare TiO_2 particles. Apparently, 1,4-butyrolactone can significantly enhance the yield stress. We shall apply our theory to fit the enhancement ratio of yield stresses, $(\tau_y - \tau_{y0})/\tau_{y0}$ [see Fig. 11(b)]. Most of the parameters we used in the numerical calculation [Fig. 11(b)] were obtained from the experiment. The amorphous x-ray pattern displayed in Fig. 2 implies that TiO_2 particles have a character that is similar to anatase. So, we take the dielectric constant of TiO_2 to be $\epsilon_1 = 31.0\epsilon_0$, the same as that of anatase. And the dielectric constant of the host medium (silicon oil) is $\epsilon_m = 2.5\epsilon_0$. The average radius, about $0.4 \mu\text{m}$, is obtained by observing the average size of the particles. And the gap between the two particles is taken to be 2 nm, which is on the same order as those in Refs. 14 and 25.

In general, the stress $\tau(\theta)$ changes with shear strain θ . The static yield stress is the maximum point in the stress–strain relation, beyond which the stress decreases as the strain increases, indicating instability. In our model, the shear angle θ does not change with the applied field, and its fixed value is 0.635. The substitution of $\theta = 0.635$ into Eq. (6) can lead to yield stresses τ_y and τ_{y0} , accordingly. The effective induced dipole moment p is made up of a number of n polar molecules (intrinsic dipoles). We set n to be linked with the Langevin function $L(E_0)$,

$$n = \alpha + \beta L(E_0) \quad (7)$$

Here, we take

$$L(E_0) = \frac{1}{3} \frac{p_0 E_{\text{loc}}(E_0)}{k_B T}, \quad (8)$$

which is the linear Langevin function when the local field is not extremely strong. For the theoretical fitting shown in Fig. 11(b), we set $\alpha = -92816$ and $\beta = 2.0891 \times 10^8$. The inset of Fig. 11(b) shows that n is linearly related to external electric fields according to Eq. (7), which reveals that when the applied field increases the number of polar molecules (dipoles) that change their direction to be along the local field increase proportionally. According to the linear relation predicted by Eq. (7), the inset of Fig. 11(b) displays the theoretical fitting with the experiment data. Good agreement between experiment and theory is indeed shown. According to the data on density in our experiment, we can estimate the average total

number of polar molecules adsorbed on one TiO₂ particle, which is about 2.86×10^9 . For the present fitting, the number of polar molecules (dipoles) is generally three orders of magnitude less than that. Because some 1,4-butyrolactone molecules are not located at the gap (the effects of those beyond the gap can be neglected due to symmetry, as mentioned above), we believe that the values we used are reasonable. In a word, our theory reveals that enough polar molecules (about 10^6) oriented within the field-directed gap between the colloidal particles can unexpectedly strengthen colloidal electrostatic interactions, thus yielding the unusual enhancement of yield stresses.

VI. DISCUSSION AND CONCLUSIONS

In this work, we have taken the gap to be 2 nm for model calculations. Here, we would like to give some evidence to support this value. We noticed that in Ref. 14 the authors took a transmission electron microscopy (TEM) image of nanoparticles in a giant ER suspension (see Fig. 1 in that study). The coated particle system they used is similar to ours. And in their TEM image, one can easily find that the gap between the two cores is roughly 2 nm (including the coating thickness). The parameter in our experiment has the same order as theirs. Thus, we have taken the gap to be 2 nm for model calculations.

In this study, we have chosen TiO₂ and achieved its ER enhancement under dc electric fields by doping 1,4-butyrolactone through the sol-gel technique. The yield stress of the ER fluids of amorphous TiO₂ modified by 1,4-butyrolactone suspended in silicon oil reaches 48.1 kPa under a dc external field of 5 kV/mm, and the current density is $<14 \mu\text{A}/\text{cm}^2$. The sedimentation ratio of the prepared ER fluids with a liquid–solid ratio of 0.45 mL/g is almost unnoticeable within approximately 20 days. The good agreement between experiment and theory shows quantitatively that enough polar molecules oriented within the field-directed gap between the colloidal particles can unexpectedly enhance colloidal electrostatic interactions, thus yielding the unusual enhancement of yield stresses. This work shows a promising and flexible direction for achieving more highly active ER materials.

ACKNOWLEDGMENTS

We thank Prof. K.Q. Lu, Ms. R. Shen, Prof. F. Lu, and Mr. C.X. Wang for fruitful discussion and help. This work was supported by the National Natural Science Foundation of China under Grant Nos. 10574027 and 10604014, and by the Science Creative Foundation (B2-13-08) of Fudan University. W.J. Tian and J.P. Huang also acknowledge financial support by the Shanghai Education Committee and the Shanghai Education De-

velopment Foundation (the “Shu Guang” project), by the Pujiang Talent Project (No. 06PJ14006) of the Shanghai Science and Technology Committee, and by the Chinese National Key Basic Research Special Fund under Grant No. 2006CB921706.

REFERENCES

1. J. Li, D.L. Dai, X.D. Liu, Y.Q. Lin, Y. Huang, and L. Bai: Preparation and characterization of self-formed CoFe₂O₄ ferrofluid. *J. Mater. Res.* **22**, 886 (2007).
2. J. Thessing, J.H. Qian, H.Y. Chen, N. Pradhan, and X.G. Peng: Interparticle influence on size/size distribution evolution of nanocrystals. *J. Am. Chem. Soc.* **129**, 2736 (2007).
3. C.W. Cho, S.K. Kim, U. Paik, J.G. Park, and W.M. Sigmund: Atomic force microscopy study of the role of molecular weight of poly(acrylic acid) in chemical mechanical planarization for shallow trench isolation. *J. Mater. Res.* **21**, 473 (2006).
4. Y.C. Weng, L. Rusakova, A. Baikalov, J.W. Chen, and N.L. Wu: Microstructural evolution of nanocrystalline magnetite synthesized by electrocoagulation. *J. Mater. Res.* **20**, 75 (2005).
5. U.T. Gonzenbach, A.R. Studart, E. Tervoort, and L.J. Gauckler: Ultrastable particle-stabilized foams. *Angew. Chem., Int. Ed. Engl.* **45**, 3526 (2006).
6. J. Wang, D.Y. Wang, N.S. Sobal, M. Giersig, M. Jiang, and H. Mohwald: Stepwise directing of nanocrystals to self-assemble at water/oil interfaces. *Angew. Chem., Int. Ed. Engl.* **45**, 7963 (2006).
7. X.W. Zhao, Y. Cao, F. Ito, H.H. Chen, K. Nagai, Y.H. Zhao, and Z.Z. Gu: Colloidal crystal beads as supports for biomolecular screening. *Angew. Chem., Int. Ed. Engl.* **45**, 6835 (2006).
8. D.S. Zhou, J.F. Zhang, L. Li, and G. Xue: Control of the geometry of the adsorbed thin layer by the depletion interaction. *J. Am. Chem. Soc.* **125**, 11774 (2003).
9. T.C. Halsey: Electrorheological fluids. *Science* **258**, 761 (1992).
10. T. Hao: Electrorheological fluids. *Adv. Mater.* **13**, 1847 (2001).
11. Y.L. Zhang, K.Q. Lu, G.H. Rao, Y. Tian, S. Zhang, and J.K. Liang: Electrorheological fluid with an extraordinarily high yield stress. *Appl. Phys. Lett.* **80**, 888 (2002).
12. R. Tao and J.M. Sun: 3-dimensional structure of induced electrorheological solid. *Phys. Rev. Lett.* **67**, 398 (1991).
13. M. Whittle and W.A. Bullough: Materials science: The structure of smart fluids. *Nature* **358**, 373 (1992).
14. W.J. Wen, X.X. Huang, S.H. Yang, K.Q. Lu, and P. Sheng: The giant electrorheological effect in suspensions of nanoparticles. *Nat. Mater.* **2**, 727 (2003).
15. J.B. Yin and X.P. Zhao: Giant electrorheological activity of high surface area mesoporous cerium-doped TiO₂ templated by block copolymer. *Chem. Phys. Lett.* **398**, 393 (2004).
16. T. Yogo, T. Yamamoto, W. Sakamoto, and S. Hirano: In situ synthesis of nanocrystalline BaTiO₃ particle-polymer hybrid. *J. Mater. Res.* **19**, 3290 (2004).
17. B.X. Wang and X.P. Zhao: Wettability of bionic nanopapilla particles and their high electrorheological activity. *Adv. Funct. Mater.* **15**, 1815 (2005).
18. W.Y. Tam, G.H. Yi, W.J. Wen, H.R. Ma, M.M.T. Loy, and P. Sheng: New electrorheological fluid: Theory and experiment. *Phys. Rev. Lett.* **78**, 2987 (1997).
19. W.J. Wen, X.X. Huang, and P. Sheng: Particle size scaling of the giant electrorheological effect. *Appl. Phys. Lett.* **85**, 299 (2004).
20. M.S. Cho, H.J. Choi, and M.S. Jhon: Shear stress analysis of a semiconducting polymer based electrorheological fluid system. *Polymer* **46**, 11484 (2005).

21. T. Hao: The interfacial polarization-induced electrorheological effect. *J. Colloid Interface Sci.* **206**, 240 (1998).
22. T. Hao, A. Kawai, and F. Izkaki: Mechanism of the electrorheological effect: Evidence from the conductive, dielectric, and surface characteristics of water-free electrorheological fluids. *Langmuir* **14**, 1256 (1998).
23. W.J. Wen, N. Wang, W.Y. Tam, and P. Sheng: Magnetic materials-based electrorheological fluids. *Appl. Phys. Lett.* **71**, 2529 (1997).
24. Y.M. Jiang and M. Liu: Energetic instability unjams sand and suspension. *Phys. Rev. Lett.* **93**, 148001 (2004).
25. K.Q. Lu, R. Shen, X.Z. Wang, G. Sun, W.J. Wen, and J.X. Liu: Polar molecule dominated electrorheological effect. *Chin. Phys. Lett.* **15**, 2476 (2006).
26. M. Sasidharan, N.K. Mal, and A. Bhaumik: In-situ polymerization of grafted aniline in the channels of mesoporous silica SBA-15. *J. Mater. Chem.* **17**, 278 (2007).
27. W.J. Tian, T. Nakayama, J.P. Huang, and K.W. Yu: Scaling behaviors in settling process of fractal aggregates in water. *Europhys. Lett.* **78**, 46001 (2007).
28. M.C. Qi and M.T. Shaw: Sedimentation-resistant electrorheological fluids based on PVAL-coated microballoons. *J. Appl. Polym. Sci.* **65**, 539 (1997).
29. M. Shen, J.G. Cao, H.T. Xue, J.P. Huang, and L.W. Zhou: Structure of polydisperse electrorheological fluids: Experiment and theory. *Chem. Phys. Lett.* **423**, 165 (2006).
30. G.Q. Gu, K.W. Yu, and P.M. Hui: A theory of induced interaction between rotating particles in electrorheological fluids. *J. Chem. Phys.* **116**, 24 (2002).
31. H.J. Choi, M.S. Cho, J.W. Kim, C.A. Kim, and M.S. Jhon: A yield stress scaling function for electrorheological fluids. *Appl. Phys. Lett.* **78**, 3806 (2001).